10th International Symposium on the Science and Processing of Cast Iron – SPCI10

A Study of the Oxygen Activity before Start of Solidification of Cast Irons

J.Ekengård[1*], A.Diószegi[2], P.G. Jönsson[3]
[1] Sandvik SRP AB, Svedala, Sweden
[2] Jönköping University, School of Engineering, Dept. of Materials and Manufacturing – Foundry Technology, P.O. Box 1026, SE-551 10 Jönköping, Sweden
[3] Royal Institute of Technology, School of Industrial Engineering and Management, Material Science and Engineering, Div. of Applied Process Metallurgy, Stockholm, Sweden.

In the present paper the oxygen balance during a temperature decrease and especially at temperatures close to the liquidus temperature has been studied for lamellar, compacted and nodular cast irons. Extrapolated data from the full scale trial results show that there are significant differences in the level of dissolved oxygen before start of solidification. Earlier research suggest the influence of the dissolved oxygen on the graphite shape, while the present work draws the attention on how the different shaped lamellar-, compacted- and nodular graphite is incorporated in the austenite matrix based on the differences in the dissolved oxygen content. Predicted differences in the dissolved oxygen are also suggested to influence the growth mechanism of the eutectic colonies and the graphite morphologies in the lamellar cast irons.

Key words: austenite, primary dendrite, lamellar graphite, compacted graphite, nodular graphite, oxygen.

Introduction

General considerations of the total and dissolved oxygen in cast iron

Oxygen in liquid cast iron, can exist as dissolved oxygen or in oxides. The sum of these two contributions gives the total oxygen content. In addition, during a temperature decrease, the dissolved oxygen is also combined with alloying elements to form non-metallic or gaseous compounds[1]. The dissolved oxygen causes changes in the interfacial energy in the solid-liquid interface during solidification and therefore it also influences the crystal growth of graphite[2]. The oxygen combined as oxides is related to a heterogeneous nucleation and a slag formation[3]. This is both advantageous and disadvantageous, due to that oxygen first assists in the nucleation of graphite during solidification. Thereafter, if the poured melt is not raked or filtered properly, it can cause surface or internal defects in the cast product.

The formation of oxides during melting is influenced by a number of factors such as melt surface properties, refractory conditions, melt temperature and melt composition. In the processing of steel, oxygen activity measurements and slag analyses are used as a tool to refine the melt properties. Therefore, the question is if this also is the road towards cast irons with stable properties? One challenge is that industrial cast iron melts are more or less supersaturated with oxygen, due to a contact with the atmosphere. Therefore, the melt contains more oxygen than would otherwise be present at equilibrium.[4]

The influence of dissolved oxygen on the nucleation and growth morphology in cast iron.

The dissolved oxygen plays a decisive role in controlling the graphite morphology. According to [5.6] oxygen atoms and other surface active elements are absorbed on the prism plan of the graphite lattice which block growth in the c-direction. A consequence is a preferred growth in a-direction and a resulting lamellar morphology of the graphite. A removal of dissolved oxygen and other surface active elements like sulphur would enable a graphite growth in the c-direction.

The morphologies of compacted and nodular iron are controlled by surface active elements such as oxygen. Also, lamellar cast iron has a large variety of graphite morphologies and consequently a large variation of the thermo mechanical and thermo physical properties. From the literature [7] it is known that additions of small amounts of deoxidizing elements, less than necessary to form compacted graphite iron, causes the bended shape of the lamellar graphite to transform to a straight shape. Furthermore, to promote higher heat conductivity in the flake graphite iron.

Scope of the present paper

The scope of the present investigation was to measure the dissolved oxygen content during melting and preparation of the liquid iron to cast components, resulting in different graphite morphologies. Due to limitations on the measurement techniques for the temperature ranges close to the solidification temperature, the obtained values were extrapolated towards the liquidus temperatures. This enabled a prediction of the dissolved oxygen levels at nucleation and growth of different cast iron grades.

* Corresponding author, e-mail: johan.ekengard@sandvik.com

Experimental Procedure

Plant trials were performed at three occasions, two lamellar cast iron experiments at Foundry 1 (F1) and another experiment at Foundry 2 (F2) with lamellar, compacted and nodular iron melts.

Process and sampling descriptions

At F1, grey iron melts with different carbon contents were prepared in a six-tonne medium frequency induction furnace. Each trial started with a molten iron, a turned off power and a starting temperature of 1500^{o}C. The raw material for the charges at F1 was machined chip. Iron samples, top slag samples, oxygen activity measurement, and temperature were all taken during 10-15 sampling occasions. Iron samples were sampled with scoop and poured into a cleaned copper mould. Top slag samples were sampled with scoop and poured onto a clean steel plate. Oxygen activity measurements were conducted with a Heraeus ElectroNite MultiLab Celox with probes for cast iron. The temperature was measured with a Heraeus ElectroNite temperature probe. When the temperature was below 1250 ^{o}C to 1270 ^{o}C the measurement was finished and the power was turned on again.

At F2 a lamellar cast iron (LGI) melt was prepared in a six-tonne furnace. After a complete melting the power was turned off. The raw materials for the charges at F2 consisted of returned plate and cast iron returns. Sampling of the same type with same technique as in the F1 experiment were conducted every 10 minutes. The melt was reheated and used as a base iron for Mg-treatment. Four Mg treatments were carried out, two aiming to produce nodular (SGI) iron and another two aiming to produce compacted (CGI) iron. The same base iron melt was used for all four Mg treatments.

Results and Discussion

Primary results

Table 1 in the Appendix shows the sampling temperature range and the determined chemical compositions. The first four experiments called LGI 28, LGI 32, LGI 34 and LGI 37 were conducted at Foundry 1, and the LGI 35 together with the CGI and SGI experiments were conducted at Foundry 2.

Dissolved oxygen in non-treated liquid iron

The temperature dependence of the oxygen activity, $a_{\underline{O}}$, has been evaluated by a number of authors[1-3]. A linear relationship has been proposed as

$$\log a_{\underline{O}} = C_1 \frac{1}{T} + C_2 \qquad (1)$$

where C_1 is proportional to the standard enthalpy change of the reduction or oxidation reaction taking place and C_2 is dependent on the chemical composition[2]. Furthermore, T is the temperature. In Fig. 1 results from the present work are plotted together with results from some previous studies. One hypothesis from earlier work[1] was that a higher carbon equivalent (CE) would decrease the measured oxygen activity. This trend can be seen in Fig. 1 to some extent in the previous work, but cannot be confirmed based on the results from the present study. In Fig. 1 the Kusakawa results seems differentiated with respect to the oxygen activity when varying the carbon equivalent. Mampaey´s results have a similar CE range as Kusakawa´s experiments, but differ in slope. Elmqvist´s results are based on lower CE values and consequently according to[1] should give higher oxygen activities. In the results from the present work, the differentiation of oxygen activities due to carbon equivalent cannot be repeated.

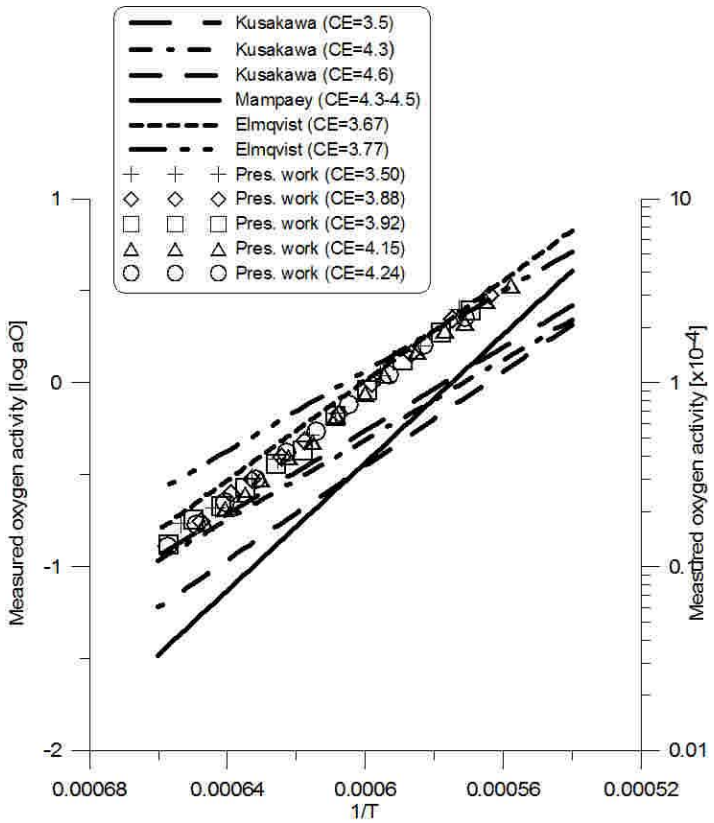

Fig. 1. Oxygen activity*) in non treated liquid iron.

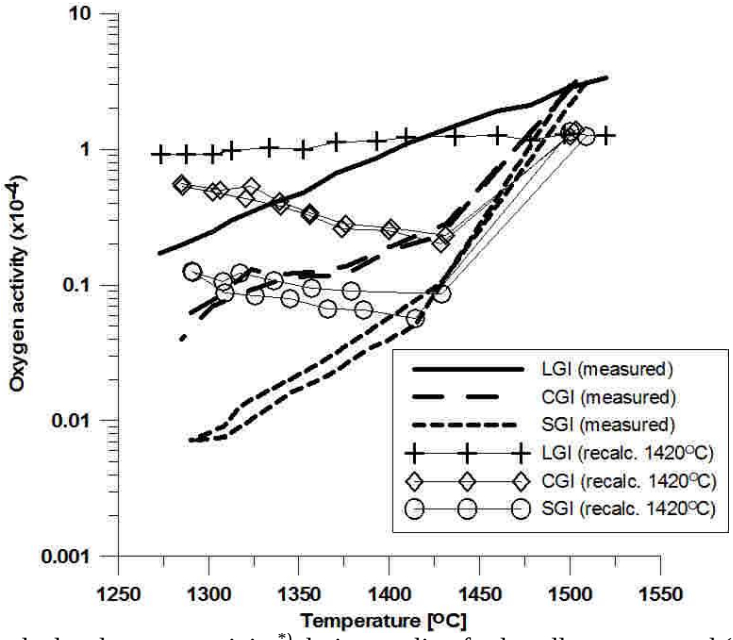

Fig.2. Measured and recalculated oxygen activity*) during cooling for lamellar, compacted (two series) and nodular (two series) cast iron melts.

Dissolved oxygen in treated liquid iron

Due to that the oxygen activity is strongly temperature dependent; Mampaey[2] recalculated measured oxygen activity values to a constant reference temperature of 1420°C. Then this value was chosen as a common casting temperature for nodular iron. The recalculated oxygen activity was retrieved using the coefficient C_1 at the measured temperature and iterating a hypothetical oxygen activity at 1420°C. This procedure was also performed in the present work as shown in Fig. 2, where the measured and the recalculated values of the oxygen activity are given. For lamellar cast iron (LGI), the recalculation only gives a view of how much the temperature influences the oxygen activity value. But for compacted graphite (CGI) and nodular iron (SGI), the recalculation reveals that the oxygen activity increases towards equilibrium as the treated melt is being cooler and at the same time the magnesium decreases in the melt. The recovery of oxygen activity due to a MgO flotation, or the effect of oxygen activity increases as the temperature decreases. In the

*) reference state 1% (by weight) hypothetical solution

everyday foundry practice this phenomena is called fading. After too long time spent between the treatment and casting the oxygen content increase. Therefore the obtained graphite morphology is different from the expected. The speed of the oxygen recovery is highly dependent on the temperature, shape and size of the ladle and whether the top slag is removed or not. The effect of a MgO flotation is partially demonstrated in Fig. 3a-b. Specifically this effect can be seen in the SGI 2 and CGI 2 series, where the MgO content in the top slag increases with a decreased temperature and the Mg content in the liquid iron decreases with a decreased temperature. Unfortunately, the SGI 1 and CGI 1 show the opposite results for MgO in the top slag, which could be due to difficulties at the top slag sampling.

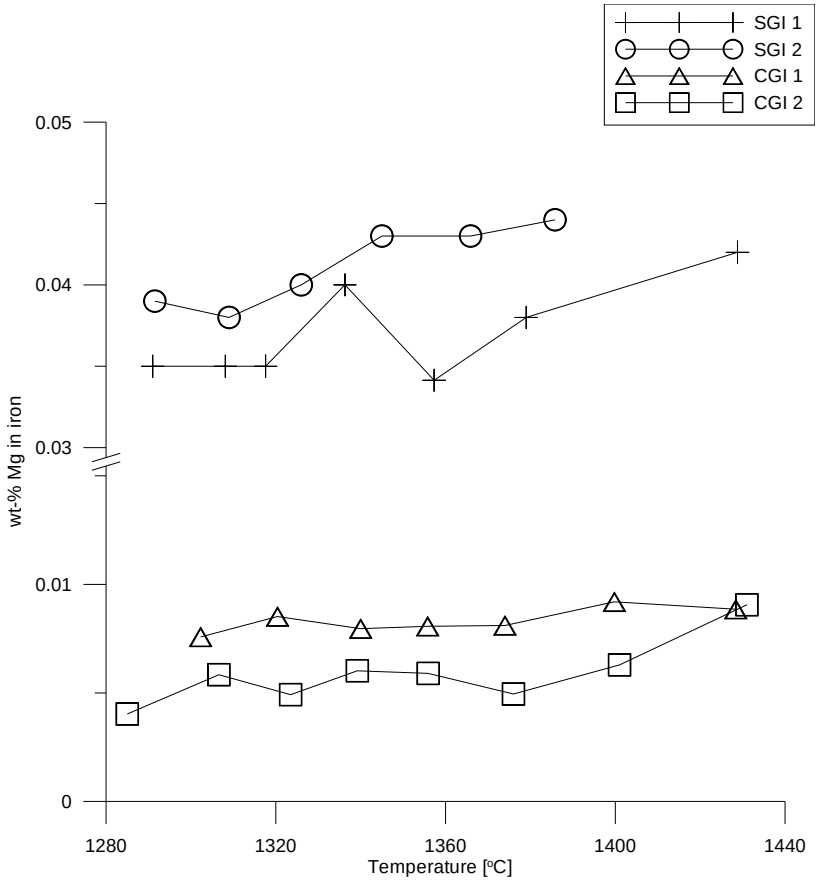

Fig.3a. Mg content in Mg treated iron in the ladle. Data are given for four trials, see Table 1.

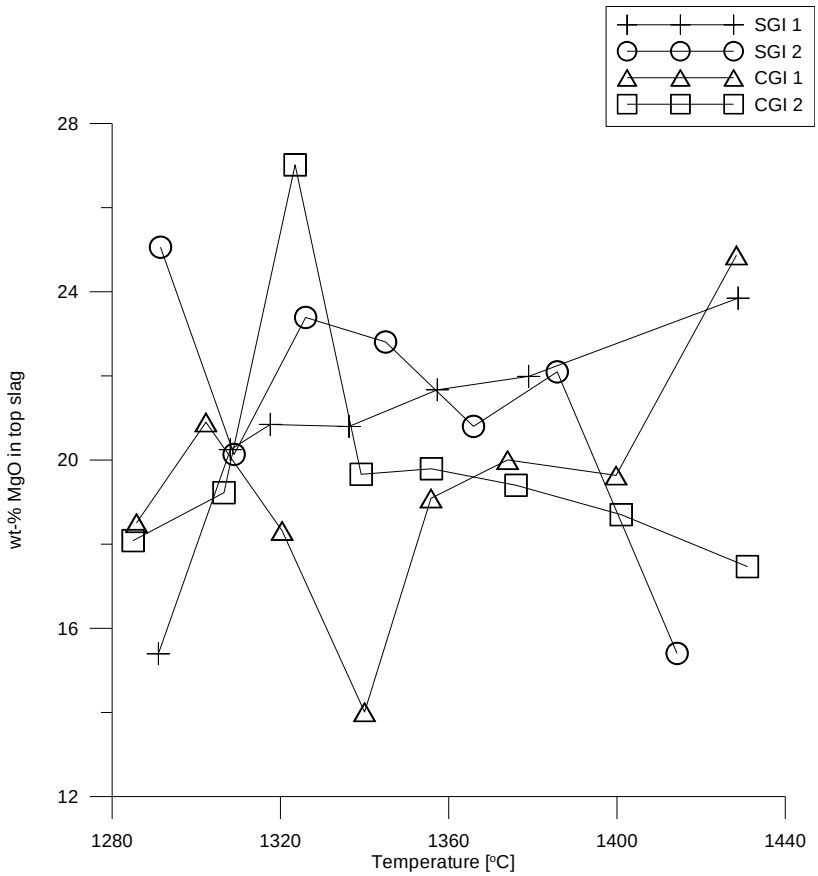

Fig.3b. MgO content in the top slag. Data are given for four trials, see Table 1.

Prediction of the dissolved oxygen content

In Fig. 4 the measured oxygen activity as function of temperature has been extrapolated towards the liquidus temperature for each iron composition. A very clear difference in oxygen activity is predicted for the different liquid irons aimed to produce nodular, compacted and lamellar cast iron. The predicted oxygen activity values support well the theories on the mechanism of graphite shape formation, where it is stated that the absence of oxygen allow the nodular graphite growth. Increasing oxygen activities contribute to a transition from nodular to compact and lamellar graphite shape.

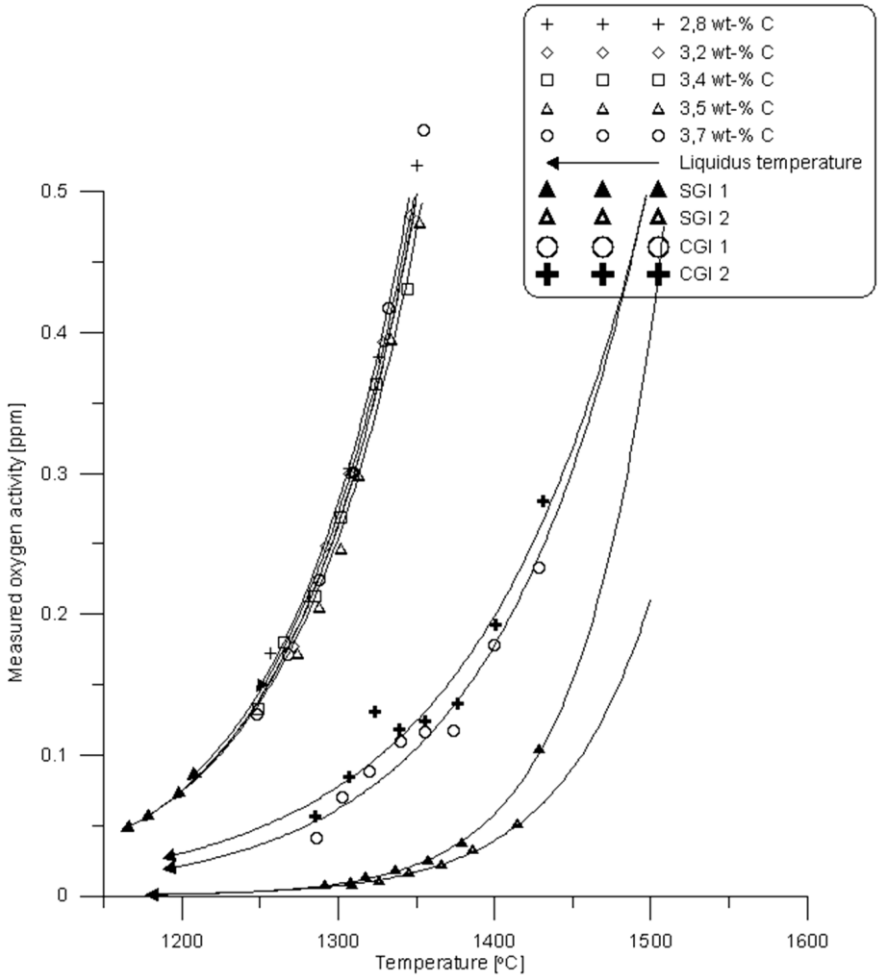

Fig.4. Extrapolated oxygen activities to liquidus temperatures.

Oxygen is considered as a surface active element, which influences the solid-liquid interfacial energy between the austenite and the liquid[8]. Consequently, it is suggested by the authors that the oxygen activity influences not only the shape of the graphite but also how the graphite particles are incorporated in the eutectic austenite during the eutectic growth. Here, nodular graphite is completely incorporated in the austenite shell[9] while compacted and lamellar graphite is incorporated only partially. That results in a cooperative growth between graphite and austenite, where the graphite remain in contact with the liquid iron.

This cooperative growth could be explained with the oxygen activity in the solidification front, where there is a gradient of surface active oxygen in the solidification range. This is due to the diffusion of carbon in the mushy zone, as can be explained with Fig. 5. A higher carbon content results in lower surface active oxygen content at the solidification front. In Fig. 4 the measured oxygen activity as function of temperature has been extrapolated to the respective liquidus temperatures. The oxygen activities almost coincide at these temperatures but the difference in the oxygen activity at the start of solidification for different carbon contents is up to 0.1 ppm. This can be seen more clearly in Fig 5. for the lamellar cast iron melts.

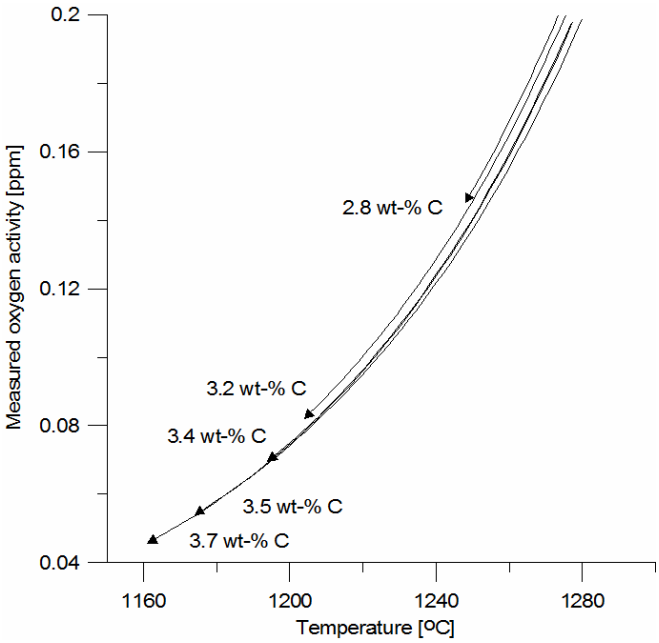

Fig.5. Extrapolated oxygen activities to liquidus temperature for lamellar cast iron melts.

The presented results of this paper were obtained from experiments where no additions of inoculants were made. In the daily foundry practice it is widespread the addition of inoculants with the scope to control the graphite nucleation[10]. Many of the inoculants include strong oxidizing element like Al, Zr, Ti, which promote oxide formation and a consequent change of the oxygen activity at the start of the solidification. In previous work[11] it has been demonstrated that the addition of inoculants containing oxidizing elements influence the number of nucleated eutectic colonies. Moreover, also the growth rate of the eutectic colonies is influenced in the case of casting of lamellar graphite iron. If we consider the growth rate of a eutectic colony proportional to the incorporation ability of graphite in to the austenite matrix, it is possible to conclude that the local oxygen activity in the solid –liquid interface control also the eutectic solidification of lamellar cast iron.

Differences in the lamellar graphite shape morphology can also be related to the oxygen content of the liquid phase. From the literature[7] it is known that additions of small amounts of deoxidizing elements, less than necessary to form compacted graphite iron, causes the bended shape of the graphite to transform to a straight shape and promote higher heat conductivity in the flake graphite iron. The present observations reveal that a lower oxygen activity can be the reason why the lamellar growth is promoted to an extreme, before the transition to a compacted shape takes place.

Conclusions

Measurements of oxygen activities indicate a large variety of dissolved oxygen levels during the processing of cast iron. In addition, clear differences in oxygen content can be predicted for different cast iron melts at temperatures close to the liquidus temperature. The lowest dissolved oxygen content is predicted for nodular cast iron melts, followed by the compacted and lamellar cast iron melts. The latter have the highest predicted dissolved oxygen level. Recalculations of the oxygen activity indicate an increase of the ”relative” oxygen activity and indicate when the treated liquid irons lose their ability to form compacted or nodular graphite. Considerable differences in oxygen activity are predicted at the liquidus temperature for different hypoeutectic iron compositions aimed for a lamellar graphite iron production. The predicted differences of the dissolved oxygen levels are suggested to be an influential factor for how graphite particles are incorporated in the austenite matrix. In the case of lamellar cast iron, the predicted differences of oxygen level are supposed to influence the morphology of the graphite lamella. Hence, the material properties like heat conductivity will be influenced.

References

[1] T. Kusakawa, X. Xu, and S. Okimoto, ‘Effects of oxygen in cast iron during melting and solidification process’, Report of the castings research laboratory, Waseda University, 1988.

[2] F. Mampaey et al.: *Giessereiforschung*, 2008, 60(1), 2-19.

[3] L. Elmquist, J. Orlenius, A. Diószegi: *Transactions of the American Foundry Society*, 2007, 115, 625-636.

[4] B. Marincek: 2nd International Symposium on ´The Metallurgy of Cast Iron´, Geneva, Switzerland 1974.

[5] B. Lux: *AFS Cast Metals Research Journal*, 1972, June, 49-65.

[6] R. Källbom: ‘Chunky graphite in heavy section ductile iron castings’, Report 16, Chalmers University of Technology, Sweden, 2006.

[7] D. Holmgren, A. Dioszegi, I.L. Svensson: *International Journal of Cast Metals Research*, 2006, 19, 6, 303-313.
[8] Z. Yuzhen, S. Yaowo and L. Yongping: *Metallurgical and Materials Transactions B*, 2006, 37B, 485–493.
[9] G.L. Rivera, R. Boeri and J Sikora: Proceedings of the Eight International Symposium on 'Science and Processing of Cast Iron', Beijing, China 2006.
[10] I.L. Svensson, A. Millberg, A. Diószegi: *Journal of Cast Metals Research*, 2003, 16, 29-34.
[11] A. Diószegi: 'On the Microstructure Formation and Mechanical Properties in Grey Cast Iron', Dissertation 871, Linköping Studies in Science and Technology, Sweden, 2004.

Acknowledgement

The present work was performed within the frame of IEC/CIC which is collaboration between Jönköping University, Swerea Swecast, and Swedish foundries. Special thanks are expressed for SKF Mekan AB and Volvo Powertrain AB hosting the experiments and Camelia Bondesson and Vasilios Fourlakidis for assistance during the experimental procedure.

Appendix 1

Table 1. Iron analyses and temperatures

		Temp [C]	C	Si	Mn	P	S	Cr	Ni	Mo	Cu	Sn	Al	Ti
								[wt-%]						
	min	1257	2,83	1,91	0,58	0,026	0,055	0,182	0,059	0,202	0,83	0,047	0,002	0,010
LGI 28	max	1473	2,87	1,96	0,59	0,027	0,061	0,184	0,061	0,205	0,85	0,047	0,002	0,011
	stddev		0,01	0,02	0,00	0,000	0,002	0,001	0,000	0,001	0,00	0,000	0,000	0,000
	min	1271	3,21	1,90	0,56	0,026	0,052	0,179	0,059	0,199	0,83	0,046	0,002	0,010
LGI 32	max	1500	3,26	1,92	0,57	0,027	0,058	0,181	0,061	0,202	0,83	0,047	0,002	0,010
	stddev		0,02	0,01	0,00	0,000	0,002	0,001	0,000	0,001	0,00	0,000	0,000	0,000
	min	1249	3,28	1,71	0,59	0,033	0,061	0,151	0,048	0,220	0,88	0,055	0,002	0,012
LGI 34	max	1483	3,40	1,72	0,60	0,035	0,073	0,153	0,049	0,226	0,88	0,057	0,002	0,012
	stddev		0,03	0,00	0,00	0,001	0,003	0,000	0,000	0,002	0,00	0,001	0,000	0,000
	min	1248	3,55	1,75	0,58	0,034	0,064	0,159	0,050	0,221	0,87	0,045	0,002	0,012
LGI 37	max	1478	3,72	1,78	0,60	0,036	0,073	0,161	0,051	0,226	0,88	0,046	0,002	0,013
	stddev		0,05	0,01	0,00	0,001	0,003	0,001	0,000	0,002	0,00	0,001	0,000	0,000
	min	1274	3,46	1,87	0,62	0,014	0,045	0,036	0,035	0,007	0,85	0,006	0,003	0,005
LGI 35	max	1534	3,57	1,89	0,63	0,016	0,052	0,036	0,036	0,008	0,86	0,007	0,003	0,005
	stddev		0,03	0,01	0,00	0,000	0,002	0,000	0,000	0,000	0,00	0,000	0,000	0,000
	min	1286	3,05	1,39	0,38	0	0,008	0,026	0,032	0,003	0,28	0,005	0,003	0,003
CGI 1	max	1503	3,56	2,16	0,39	0	0,009	0,026	0,033	0,006	0,28	0,006	0,005	0,005
	stddev		0,16	0,26	0,00	0	0,000	0,000	0,000	0,001	0,00	0,000	0,001	0,000
	min	1285	3,07	1,38	0,37	0	0,007	0,026	0,032	0,003	0,28	0,005	0,003	0,003
CGI 2	max	1500	3,51	2,12	0,39	0	0,009	0,026	0,033	0,003	0,28	0,005	0,005	0,004
	stddev		0,15	0,24	0,00	0	0,001	0,000	0,000	0,000	0,00	0,000	0,001	0,000
	min	1291	3,38	1,42	0,39	0	0,007	0,027	0,032	0,003	0,28	0,005	0,003	0,004
SGI 1	max	1509	3,55	2,10	0,40	0	0,008	0,027	0,033	0,003	0,28	0,005	0,009	0,005
	stddev		0,06	0,24	0,00	0	0,001	0,000	0,000	0,000	0,00	0,000	0,002	0,000
	min	1292	3,34	1,39	0,38	0	0,006	0,026	0,032	0,003	0,28	0,005	0,003	0,003
SGI 2	max	1500	3,49	2,16	0,40	0	0,008	0,027	0,033	0,003	0,28	0,005	0,009	0,005
	stddev		0,05	0,29	0,01	0	0,000	0,000	0,000	0,000	0,00	0,000	0,002	0,000